VTT PUBLICATIONS 304

Theoretical studies on aerosol agglomeration processes

Kari E. J. Lehtinen

VTT Energy

Dissertation for the degree of Doctor of Technology to be presented with permission for public examination and depate in Auditorium E at Helsinki University of Technology (Espoo, Finland) on the 26th of April, 1997, at 12 o'clock noon.

TECHNICAL RESEARCH CENTRE OF FINLAND
ESPOO 1997

ISBN 951-38-5047-1 (soft back ed.)
ISSN 1235-0621 (soft back ed.)

ISBN 951-38-5048-X (URL: http://www.inf.vtt.fi/pdf/)
ISSN 1455-0849 (URL: http://www.inf.vtt.fi/pdf/)

JULKAISIJA – UTGIVARE – PUBLISHER

Valtion teknillinen tutkimuskeskus (VTT), Vuorimiehentie 5, PL 2000, 02044 VTT
puh. vaihde (09) 4561, faksi (09) 456 4374

Statens tekniska forskningscentral (VTT), Bergsmansvägen 5, PB 2000, 02044 VTT
tel. växel (09) 4561, fax (09) 456 4374

Technical Research Centre of Finland (VTT), Vuorimiehentie 5, P.O.Box 2000, FIN–02044 VTT, Finland
phone internat. + 358 9 4561, fax + 358 9 456 4374

VTT Energia, Energian käyttö, Biologinkuja 7, PL 1401, 02044 VTT
puh. vaihde (09) 4561, faksi (09) 460 7021
VTT Energi, Energiandvändning, Biologgränden 7, PB 1401, 02044 VTT
tel. växel (09) 4561, fax (09) 460 7021
VTT Energy, Energy Use, Biologinkuja 7, P.O.Box 1401, FIN–02044 VTT, Finland
phone internat. + 358 9 4561, fax + 358 9 460 7021

Technical editingLeena Ukskoski

LIBELLA PAINOPALVELU OY, ESPOO 1997

Lehtinen, Kari E. J. Theoretical studies on aerosol agglomeration processes. Espoo 1997. Technical Research Centre of Finland, VTT Publications 304. 45 p. + app. 89 p.

UDC 541.182.2/.3
Keywords aerosols, aerosol dynamics, electrical agglomeration, agglomerates, particle collisions, coalescence, nanomaterials

Abstract

In this thesis, theoretical modeling of certain aerosol systems has been presented. At first, the aerosol general dynamic equation is introduced, along with a discretization routine for its numerical solution. Of the various possible phenomena affecting aerosol behaviour, this work is mostly focused on aerosol agglomeration. The fundamentals of aerosol agglomeration theory are thus briefly reviewed. The two practical applications of agglomeration studied in this thesis are flue gas cleaning using an electrical agglomerator and nanomaterial synthesis with a free jet reactor.

In an electrical agglomerator the aerosol particles are charged and brought into an alternating electric field. The aim is to remove submicron particles from flue gases by collisions with larger particles before conventional gas cleaning devices that have a clear penetration window in the problematic 0.1 - 1 μm size range. A mathematical model was constructed to find out the effects of the different system parameters on the agglomerator's performance. A crucial part of this task was finding out the collision efficiencies of particles of varying size and charge. The original idea was to use unipolar charging of the particles, and a laboratory scale apparatus was constructed for this purpose. Both theory and experiments clearly show that significant removal of submicron particles can not be achieved by such an arrangement. The theoretical analysis further shows that if the submicron particles and the large collector particles were charged with opposite polarity, significant removal of the submicron particles could be obtained.

The second application of agglomeration considered in this thesis is predicting/controlling nanoparticle size in the gas-to-particle aerosol route to material synthesis. In a typical material reactor, a precursor vapor reacts to form molecules of the desired material. In a cooling environment, a particulate phase forms, the dynamics of which are determined by the rates of collisions and coalescence. In the thesis, it is first theoretically demonstrated how the onset of dendrite formation and primary particle size can be predicted by studying the characteristic time scales of collision and coalescence.

Then it is shown how the linear rate law for coalescence can be approximately applied to agglomerate structures by dividing the agglomerates into sections. The developed models are then applied to a free jet material reactor. From the comparisons between theory and experiment it is obvious that such a model is able to capture the effects of the system parameters (temperature, velocity, volume loading of material and location of collection) on the primary particle size of the produced material.

PREFACE

This thesis is based on studies carried out at the Aerosol Technology Group of VTT Energy and at the Air Quality and Aerosol Technology Laboratory of UCLA Department of Chemical Engineering. I wish to express my gratitude to all reseachers in both groups for a great scientific environment for such work. Especially, I am greatly indebted to the leaders of the groups, Dr. Jorma K. Jokiniemi and Prof. Sheldon K. Friedlander for their continuous and assiduous encouragement and supervision of my work. I am also very grateful to Dr. Esko Kauppinen of VTT Chemical Technology for his guidance and continuous support during my first steps in the field of aerosol science.

I dedicate my warmest thanks to the Laboratory of Computational Dynamics of Helsinki University of Technology, especially Prof. Eero-Matti Salonen and Doc. Juhani von Boehm, for their continuous encouragement and guidance throughout my studies and their useful suggestions regarding the thesis.

I am deeply indebted to the researchers involved in the experimental parts of this thesis, especially Dr. Jukka Hautanen from Tampere University of Technology for conducting the electrical agglomerator experiments and Dr. Robert Windeler from UCLA for our continuous collaboration in nanoparticle synthesis throughout my stay at UCLA.

I am also grateful to Dr. Bertram Schleicher and Mr. Jouni Pyykönen for their helpful suggestions regarding the writing of the thesis.

I am thankful to the Ministry of Trade and Industry's LIEKKI research program for funding the developing of the ABC computer code, the SIHTI research program for funding the electrical agglomeration project and to the VTT Exchange Program, IVO Research Foundation and Leo and Regina Wainstein Foundation for making my stay and work at UCLA possible.

Finally, I wish to thank my friends, my parents and other relatives and especially my beloved fiancee Tarja for their patience and understanding throughout this thesis work.

LIST OF PUBLICATIONS

This dissertation is a review of the author's work in the field of aerosol dynamics modeling. It consists of an overview and the following selection of the author's publications:

A Jokiniemi, J. K., Lazaridis, M., Lehtinen, K. E. J. and Kauppinen, E. I.
Numerical simulation of vapour-aerosol dynamics in combustion processes.
J. Aerosol Sci. 1994. Vol. 25, pp. 429 - 446.

B Hautanen, J., Kilpeläinen, M., Kauppinen, E. I., Jokiniemi, J. K. and Lehtinen, K.
Electrical agglomeration of aerosol particles in an alternating electric field.
Aerosol Sci. Tech. 1995. Vol. 22, pp. 181 - 189.

C Lehtinen, K. E. J., Jokiniemi, J. K., Kauppinen, E. I. and Hautanen, J.
Kinematic coagulation of charged droplets in an alternating electric field.
Aerosol Sci. Tech. 1995. Vol. 23, pp. 422 - 430.

D Lehtinen, K. E. J., Windeler, R. S. and Friedlander, S. K.
Prediction of nanoparticle size and the onset of dendrite formation using the method of characteristic times.
J. Aerosol Sci. 1996. Vol 27, pp. 883 - 896.

E Lehtinen, K. E. J., Windeler, R. S. and Friedlander, S. K.
A note on the growth of primary particles in agglomerate structures by coalescence.
J. Colloid and Interface Sci. 1996. Vol 182, pp. 606 - 608.

F Windeler, R. S., Friedlander, S. K. and Lehtinen, K. E. J.
Production of nanometer-sized metal oxide particles by gas phase reaction in a free jet I: experimental system and results.
Accepted for publication in Aerosol Sci. Tech.

G Windeler, R. S., Lehtinen, K. E. J. and Friedlander, S. K.
Production of nanometer-sized metal oxide particles by gas phase reaction in a free jet II: particle size and neck formation - comparison with theory.
Accepted for publication in Aerosol Sci. Tech.

AUTHOR'S CONTRIBUTION

The research reported in this dissertation has been carried out at the Aerosol Technology Group of VTT Energy in Espoo, Finland (papers A, B and C) and at the UCLA Air Quality and Aerosol Technology Laboratory in Los Angeles, California (papers D, E, F and G), where the author worked as a visiting research scientist from Aug. 1994 to Aug. 1995. Papers B and C were carried out in collaboration with the Physics Dept. of Tampere University of Technology (TUT).

Paper A deals with the ABC computer code and was written mainly by Dr. Jokiniemi. The author's contributions to the paper were programming of the multicomponent gas transport coefficients, coagulation source terms and, jointly with Dr. Jokiniemi, the discrete-nodal grid for the particle size spectrum. The author also wrote the corresponding sections of the paper. The sample calculations of paper A were performed by Dr. Lazaridis.

Electrical agglomeration is discussed in papers B and C. The author's contributions to these papers include participation in the overall planning and analyzing the results of the project, all theoretical modeling of both papers and writing paper C. Dr. Hautanen from TUT performed the experiments and wrote paper B.

Papers D, E, F and G deal with controlled nanoparticle production. The theoretical (not forgetting the guidance of Prof. Friedlander) and computational work of all the papers was done by the author, as was the writing of papers D and E. The comparisons between theoretical and experimental results in paper G were done jointly with Dr. Windeler from UCLA. The author also took part in the statistical analysis of the experimental results of paper F and assisted in writing papers F and G.

TABLE OF CONTENTS

NOMENCLATURE

a	particle surface area
A	cross-sectional area
A	constant in the agglomerate power law
b	proportionality constant in charge distribution
$\bar{c}$, g, l	shortening variables in the Fuchs collision frequency function
C	proportionality function in initial neck growth equation
C_c	slip correction factor
d	particle diameter
$\bar{d}$	mean particle diameter
D	diffusion coefficient
D_0	diffusion coefficient prefactor
D_f	fractal dimension
$\vec{e}_x, \vec{e}_y, \vec{e}_z$	cartesian unit vectors
E_{act}	activation energy for the diffusion coefficient
E_0	amplitude of electric voltage
f	frequency of alternating electric field
F	rate of collisions
k	Boltzmann's constant
m	mass concentration distribution
M	total mass concentration of particles
M	molar mass
n	degree of homogenity of a homogenous function
n	number density function
n	average number of primary particles in an agglomerate
n^m	multicomponent number density function
N	number of primary particles in an agglomerate
p	pressure
q	amount of charge
r	particle radius
r_0	primary particle radius
R	removal term
R	gas constant
R^m	multicomponent removal term
S	source term
S^m	multicomponent source term
t	time
T	temperature
u,v	particle volume
$\bar{v}$	average particle volume
v_0	primary particle volume
v_k	volume of component k in a particle
v_m	molecular volume

$\dot{v}$	condensation rate
$\dot{v}_k$	condensation rate of component k
V	control volume
w	grain boundary width
x	neck radius
$\vec{x}$	position vector
$\dot{\vec{x}}$	velocity vector
x,y,z	coordinates of position vector

α	constant in the self-preserving growth law for average volume
β	collision frequency function
δ	surface thickness
ε	collision efficiency
ε_0	permittivity of vacuum
η	size variable of the self-preserving distribution
ϕ	proportionality constant for deposition
ϕ	volume fraction of particulate matter
Φ	reduction in fine mode concentration
λ	mean free path
μ	viscosity
ρ	density
σ	surface tension
σ	factor that takes into account different charging cases
τ	residence time in agglomerator
τ_c	characteristic collision time
τ_f	characteristic fusion time
ξ	Coulomb correction factor for collision frequency function
ψ	self-preserving distribution function
θ	dimensionless excess surface area
Θ	step function

Subscripts

a	agglomerate
b	grain boundary diffusion
coll	collision
Coul	Coulomb
l	lattice diffusion
p	primary particle
s	surface diffusion
sph	spherical
1	fine particle mode
2	large particle mode

1. INTRODUCTION

Aerosols are suspensions of solid and/or liquid particles in gases. They are formed by the conversion of gases to particulate matter or by the disintegration of liquids or solids. The sizes of aerosol particles range from a few nanometers to roughly hundreds of micrometers. The understanding of the physical properties of aerosols is important in many areas of research and industry, including materials processing, air pollution control, nuclear safety, combustion engineering and cloud and atmospheric sciences.

In combustion processes aerosols may cause severe slagging and fouling problems. Air pollution aerosols can have negative effects on e.g. human health and visibility. On the other hand, aerosol routes provide a convenient way of producing nanomaterials with properties significantly differing from the normal bulk properties. Medicine can also be in the form of aerosols. The basis of the new asthma inhalators lies in knowing the penetration properties of the medicine particles into the human lung.

This overview focuses mainly on methods of modeling aerosol behaviour and covers the author's work on the subject originally reported in papers A-G. A thorough introduction to previous work in this area is omitted in this overview, since it is covered in the introduction of each paper, which are attached. Predicting aerosol behaviour requires knowledge of the particle sizes, concentration, chemical composition and morphology. Chapter 2 introduces the concept of the general dynamic equation (GDE), which is an integro-differential equation describing the time evolution of the particle size distribution. A numerical solution technique for the GDE is also discussed.

Particle collisions play an important role in aerosol dynamics, and thus also in the GDE. Chapter 3 introduces the basics of aerosol agglomeration. Agglomeration is a process, in which particles collide and stick, thus forming larger particles. If the particles coalesce into spherical form, the process is usually termed coagulation. If coalescence does not occur, agglomeration leads to the formation of dendritic structures. These dendritic structures collide with a different rate, compared with spheres of same volume. This is discussed at the end of the chapter.

The remaining chapters deal with two research problems, in which particle collisions are the most important physical process affecting the evolution of the size distribution. The first problem is an example of using aerosol methods in air pollution prevention and is discussed in Chapter 4. It has been found that many particle removal devices have a penetration window in the range 0.1 - 1 μm. One idea for removing the particles in this

problematic range is to use an electrical agglomerator, in which the particles are charged and subsequently brought into an alternating electric field. The purpose of this arrangement is to remove the submicron particles with the larger particles, resulting from collisions caused by the oscillatory motion.

The second aerosol related research problem discussed in this thesis is the possibility to produce nanoparticles in a controlled way by gas-to-particle aerosol methods, which is discussed in Chapter 5. The particles are formed by chemical reactions from the vapor phase and grow by collisions. The size and shape of the formed nanoparticles depend on the relative rates of collision and coalescence. Chapter 5 summarizes the basic theoretical models with which it is possible to predict and control the size and shape of the produced nanoparticle material.

2. THE GENERAL DYNAMIC EQUATION (GDE)

The integro-differential equation that describes the dynamic behaviour of an aerosol is usually termed the general dynamic equation for aerosols (GDE; Friedlander, 1977). In its most general form, it describes the evolution of the size distribution of aerosol particles as functions of particle size and composition, but in many applications and numerical solution routines, only the dependence on size is considered.

The processes that govern the temporal and spatial changes in the size distribution are agglomeration, growth, source and removal processes. Agglomeration is a process in which particles collide and form larger particles. The most common phenomena that cause collisions are Brownian motion, external forces and turbulence. Agglomeration will be studied in more detail in the following chapters. The growth term accounts for the increase or decrease in particle size because of condensation, evaporation or reactions of gases with particle surfaces. Examples of the source and removal processes are nucleation and deposition.

2.1. Continuous GDE for the number density function

The number density function $n = n(x, v, t)$, where $\vec{x} = x\vec{e}_x + y\vec{e}_y + z\vec{e}_z$ is the position vector and v the particle volume, is defined in such a way that $n(x, v, t)dxdydzdv$ gives the number of particles with volume between v and $v+dv$ at location $\vec{x}$ in the differential box $dxdydz$. It obeys the following partial differential equation (the GDE for aerosol particles; Friedlander, 1977)

$$\frac{\partial n}{\partial t} + \nabla \cdot (\dot{\vec{x}} n) + \frac{\partial}{\partial v}(\dot{v} n) = \left(\frac{\partial n}{\partial t}\right)_{coll} + R + S \,. \tag{2.1}$$

The left hand side is comprised of terms describing the temporal and spatial changes in the number density function as well as growth/shrinkage by condensation/evaporation. Here $\dot{\vec{x}} = \dot{\vec{x}}(\vec{x}, v, t)$ is the velocity of a particle of volume v at location x and time t. The velocity $\dot{x}$ can be set to take into account the migration velocity caused by external forces and the diffusional velocity caused by concentration gradients. Usually in simulating aerosol dynamics, however, it is sufficient to set $\dot{x}$ to be equal to the gas velocity. The first term on the right hand side describes the change in the number density function caused by particle collisions or agglomeration. The form of this term will be studied in detail in the next chapter. The last two terms $R(v,n(v),\vec{x},t)$ and $S(v,n(v),\vec{x},t)$ are the removal and source terms,

respectively. The most typical removal and source terms are deposition and nucleation.

The GDE is in its general form an integro-differential equation, since the collision terms are integrals of the size distribution function *n*. Thus, numerical solutions are practically always necessary. Paper A deals with a computer program ABC, which was written to simulate aerosol behaviour in combustion processes. The computational procedure is sectional, i.e. the size distribution is divided into a number of classes. For each size section the size of the particles is described by the midpoint of the section (for this reason the solution procedure is called a nodal point method in paper A) and there is a differential equation for the number of particles in each section. The numerical procedure is discussed in more detail in Section 2.3.

2.2 Multicomponent GDE

If the aerosol particles contain many chemical components and we wish to keep track of the composition in addition to size, a different type of number distribution is required. If the multicomponent number density function $n^m = n^m(x, v_1, v_2, ..., v_m, t)$ is defined in such a way that $n^m(x, v_1, v_2, ..., v_m, t)dxdydzdv_1dv_2...dv_m$ gives the number of particles, with the volume of component *k* between v_k and v_k+dv_k, at location x and at time *t* in the differential box $dxdydz$, the GDE becomes (Gelbard and Seinfeld, 1978):

$$\frac{\partial n^m}{\partial t} + \nabla \cdot \left(\dot{\vec{x}} n^m\right) + \sum_{k=1}^{m} \frac{\partial}{\partial v_k}\left(\dot{v}_k n^m\right) = \left(\frac{\partial n^m}{\partial t}\right)_{coll} + R^m + S^m. \qquad (2.2)$$

The collision term depends on the amounts of all chemical components through its dependence on particle size and density (see Section 3.1). Equation 2.2 can be solved numerically by dividing both the size and composition axes into discrete sections (Kim and Seinfeld, 1992). This is, however, computationally extremely expensive. Another approach is to average the compositions within each size section (Gelbard and Seinfeld, 1980; Sher and Jokiniemi, 1993). The compositions in different size sections may be different and are allowed to vary as functions of time and location, but each section is represented by only one averaged composition. Then, if we have *m* size classes and *n* chemical components, we will have *mn* differential equations to be solved. This is the method used in the ABC computer code (paper A).

2.3. Discretization of the GDE

In the ABC computer code, the flow field is approximated by a plug-flow model. The discretization of the GDE is obtained by a finite volume technique. Many of the calculations of interest are stationary. In the following, the discretization technique in such cases is presented. The discretization routines of RAFT (Im et al., 1987) and NAUA-HYGROS (Jokiniemi and Sher, 1993) have been used as bases for the model.

If the GDE is integrated over a control volume V (Figure 2.1) located at x_i, where the flow is in the positive x-direction in a tube with a cross-sectional area of $A(x)$, the following form of the stationary GDE is obtained:

$$\int_V \nabla \cdot (\dot{x} n) dV + \int_V \frac{\partial}{\partial v} (\dot{v} n) dV = \int_V \left[\left(\frac{\partial n}{\partial t} \right)_{coll} + R + S \right] dV \,. \tag{2.3}$$

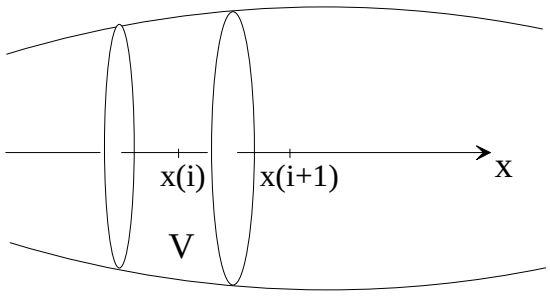

Figure 2.1. Control volume approach to discretizing the GDE.

Here it is also assumed that all the variables are independent of y and z. The first term can be transformed using Gauss's law: $\int_V \nabla \cdot (\dot{x} n) dV = \int_A (\dot{x} n) \cdot d\vec{A}$.

The (deposition) removal term R is proportional to the number density function n: $R = -\phi n$. The form of the source (nucleation) term S is discussed in paper A. If, in addition, the volume V is very thin, we can approximate $V(x_i) \approx A(x_i) \cdot \Delta x_i$ and equation 2.3 becomes:

$$\begin{aligned} &\frac{A_{i+1/2} \dot{x}_{i+1/2,j} n_{i+1/2,j} - A_{i-1/2} \dot{x}_{i-1/2,j} n_{i-1/2,j}}{A_i \Delta x_i} \\ &+ \frac{\dot{v}_{i,j+1/2} n_{i,j+1/2} - \dot{v}_{i,j-1/2} n_{i,j-1/2}}{\Delta v_j} = \left(\frac{\partial n}{\partial t} \right)_{coll,ij} - \phi_{ij} n_{ij} + S_{ij} \end{aligned} \tag{2.4}$$

The discretization of the condensation/evaporation term results from similar finite volume thinking as with the convecton term (the index j refers to the radius coordinate).

The cross-sectional areas $A_{i+1/2}$ and $A_{i-1/2}$, the particle velocities $\dot{x}_{i+1/2,j}$ and $\dot{x}_{i-1/2,j}$ as well as the particle growth rates $\dot{v}_{i,j+1/2}$ and $\dot{v}_{i,j-1/2}$ are computed at the cell boundaries using the known geometrical and physicochemical data, but the discretized size distribution is stored only at the midpoints n_{ij}. The discretized size distribution values in the convection and growth terms $n_{i+1/2,j}$, $n_{i-1/2,j}$, $n_{i,j+1/2}$ and $n_{i,j-1/2}$ are approximated by their nearest upwind values, i.e. the first order upwind discretization is used:

$$n_{i+1/2,j} \approx n_{ij} \tag{2.5}$$

$$n_{i,j+1/2} \approx \begin{cases} n_{i,j+1}, & \dot{v}_{i,j+1/2} < 0 \\ n_{ij}, & \dot{v}_{i,j+1/2} > 0 \end{cases} \tag{2.6}$$

By using the first order upwind discretizing technique, the solution method is robust and ”reasonable looking” solutions are practically always obtained. However, numerical diffusion decreases the accuracy of the solution.

The terms can now be grouped in such a way that the algebraic nature of the solution procedure can be clearly seen:

$$\begin{aligned} &\left(\phi_{ij} + \frac{A_{i+1/2}\dot{x}_{i+1/2,j}}{A_i \Delta x_i} + \frac{1}{\Delta v_j} \begin{cases} \dot{v}_{i,j+1/2} & [1] \\ -\dot{v}_{i,j-1/2} & [2] \\ \dot{v}_{i,j+1/2} - \dot{v}_{i,j-1/2} & [3] \end{cases} \right) n_{ij} \\ &= \frac{1}{\Delta v_j} \begin{cases} \dot{v}_{i,j-1/2} & [1] \\ 0 & [2] \\ 0 & [3] \end{cases} n_{i,j-1} + \frac{1}{\Delta v_j} \begin{cases} 0 & [1] \\ -\dot{v}_{i,j+1/2} & [2] \\ 0 & [3] \end{cases} n_{i,j+1} \\ &+ \left(S_{i-1,j} + \left(\frac{\partial n}{\partial t} \right)_{coll,i-1,j} + \frac{A_{i-1/2}\dot{x}_{i-1/2,j}}{A_i \Delta x_i} n_{i-1,j} \right) \end{aligned} \tag{2.7}$$

Case [1], [2] or [3] is applied according to the following criteria:

[1] $\dot{v}_{i,j+1/2} \geq 0, \dot{v}_{i,j-1/2} \geq 0$
[2] $\dot{v}_{i,j+1/2} < 0, \dot{v}_{i,j-1/2} < 0$
[3] $\dot{v}_{i,j+1/2} \geq 0, \dot{v}_{i,j-1/2} < 0$

Case [3], where some particles grow and some evaporate, is possible because of the Kelvin effect (Hinds, 1982). If the conditions are such that all particles grow, then we have case [1] for all size classes *j*. The equation for n_{ij} will then not include $n_{i,j+1}$. The solution of any matrix equations can therefore be avoided, since we can just start by solving the equation for n_{i1}, then n_{i2} and so on. If all particles evaporate and we have case [2] for all size classes, we have a similar situation, except that then we start by solving the equation for $n_{i,max}$. If there exists a size class *k* such that all particles larger than r_k grow and smaller than r_k evaporate, we start by solving for $n_{i,k}$, after which we proceed to $n_{i,k-1}$ and $n_{i,k+1}$, and so on.

This discretisation scheme, which is taken from RAFT (Im et al.,1987), is semi-implicit in nature. In stationary systems, the solution marches along the *x*-axis in small increments solving for the size distribution *n* at every *x*, at the same time keeping track of the gas phase concentrations. The other terms are treated implicitly, except for the nucleation and collision source terms, in which size distribution values at x_{i-1} are used when calculating term values at x_i.

In the modeling of aerosol dynamics it is convenient to use a sectionalization, in which the sections are evenly spaced on the logarithmic axis (v_{i+1}/v_i = constant). Sometimes, however, a more accurate model for the lower end of the size spectrum is needed and thus a discrete-sectional or discrete-nodal point discretization is more appropriate (Wu and Flagan, 1988, Paper A). This means that the size axis is divided monomer by monomer up to a certain prefixed size, after which the logarithmically even spacing is applied.

3. AGGLOMERATION OF AEROSOL PARTICLES

Agglomeration is a process in which particles collide and form larger particles. Thus, as a consequence of agglomeration the average particle size increases and the total number concentration decreases. If the collided particles coalesce to spherical form, the process is usually called coagulation. If the particles do not coalesce but stick together, dendritic agglomerates tend to form. Here we will use the term agglomeration for all collision processes that result in the particles sticking together, regardless of whether they coalesce or not. Coagulation is regarded as a special case of agglomeration, where there is instantaneous coalescence after collision.

The most common phenomena that cause collisions are Brownian motion, external forces and turbulence. In this chapter Brownian agglomeration and kinematic agglomeration caused by electrical forces are studied in more detail. The theoretical treatment of agglomeration consists of keeping count of the number of particles as a result of the collisions (Schmoluchowski, 1917) and determining the collision frequency function as a function of particle sizes, particle densities and system parameters.

As mentioned in Chapter 2, agglomeration is just one physical phenomenon affecting the time evolution of aerosol systems. Here it is studied in more detail, since it is the dominant particle growth mechanism for both the electrical agglomerator system (papers B and C) and material synthesis (papers D, E and F) processes.

3.1. The continuous agglomeration equation

Let $n(v)$ be the particle size distribution function defined in the previous chapter. Then the rate of collisions per unit volume of gas $F(u,v)$ between particles of size u and v is

$$F(u,v) = \beta(u,v)n(u)n(v)dudv \tag{3.1}$$

Here $\beta(u,v)$ is the collision frequency function. It depends on particle sizes, densities and system variables and will be introduced in more detail in the next two chapters. If particle collisions are the only phenomenon affecting the size distribution, we have the equation (Friedlander, 1977):

$$\left(\frac{\partial n(v)}{\partial t}\right)_{coll} = \frac{1}{2}\int_0^v \beta(u, v-u)n(u)n(v-u)du - \int_0^\infty \beta(u,v)n(u)n(v)du \tag{3.2}$$

The first term is the rate of formation of particles of size v by smaller particles of sizes u and v-u. The factor 1/2 must be introduced since collisions are counted twice in the integral. The second term is the rate of loss of particles of size v by collision with all other particles. The multicomponent collision terms are a simple extension to equation 3.2.

$$\left(\frac{\partial n^m(v_1,\ldots,v_m)}{\partial t}\right)_{coll} = \frac{1}{2}\int_0^{v_1}\ldots\int_0^{v_m}\beta(u_1,\ldots,u_m,v_1-u_1,\ldots,v_m-u_m)\, n^m(u_1,\ldots,u_m)n^m(v_1-u_1,\ldots,v_m-u_m)du_1\ldots du_m - \int_0^{\infty}\ldots\int_0^{\infty}\beta(u_1,\ldots,u_m,v_1,\ldots,v_m)n^m(u_1,\ldots,u_m)\, n^m(v_1,\ldots,v_m)du_1\ldots du_m. \quad (3.3)$$

In the ABC model (Paper A), the agglomeration source terms for each source term are computed by the following technique: All the particle size pairs are gone through one by one. If the size of the particle resulting from a collision falls between two nodal points, the resulting particle is divided between those nodal points in such a way that number and volume are conserved (size-splitting).

3.2. Brownian agglomeration

If particles are smaller than about 1 μm in diameter, they collide because of their Brownian motion. The collision frequency function for this mechanism can be expressed as (Fuchs, 1964):

$$\beta(u,v) = \begin{cases} \frac{2kT}{3\mu}\left(\frac{1}{u^{1/3}}+\frac{1}{v^{1/3}}\right)\left(u^{1/3}+v^{1/3}\right); & \text{continuum regime} \\ \left(\frac{3}{4\pi}\right)^{1/6}\left(\frac{6kT}{\rho_p}\right)^{1/2}\left(\frac{1}{u}+\frac{1}{v}\right)^{1/2}\left(u^{1/3}+v^{1/3}\right)^2; & \text{free molec. regime} \end{cases} \quad (3.3)$$

If the particles are large enough that they experience the surrounding gas as a continuum, the particle size is said to be in the continuum regime. Then the particle diameter is larger than the mean free path of the gas (≈ 0.07μm for air in standard conditions). If the particle diameter is much smaller than the mean free path of the surrounding gas, it is said to be in the free molecular regime. The intermediate region is usually called the transition regime.

The continuum regime expression for the collision frequency function is obtained by solving the diffusion equation of particles of volume *v* around one particle of volume *u* that is assumed to be fixed using the relative diffusion coefficient *D(u)+D(v)* (see Fuchs, 1964). The free molecular collision frequency function is an expression derived by the kinetic theory of gases assuming rigid elastic spheres. There is no simple collision frequency function for the transition regimes that could be derived "from first principles". Fuchs (1964) proposed an interpolation formula for the whole particle diameter range that has been generally accepted:

$$\beta\left(d_i, d_j\right) = \frac{2\pi\left(D_i + D_j\right)\left(d_i + d_j\right)}{\dfrac{d_i + d_j}{d_i + d_j + 2\sqrt{g_i^2 + g_j^2}} + \dfrac{8\left(D_i + D_j\right)}{\sqrt{\bar{c}_i^2 + \bar{c}_j^2}\left(d_i + d_j\right)}} \tag{3.4}$$

where

$$D_i = \frac{kTC_c\left(d_i\right)}{3\pi\mu d_i}, \qquad \bar{c}_i = \sqrt{\frac{8kT}{\pi m_i}}, \qquad g_i = \frac{\left(d_i + l_i\right)^3 - \left(d_i^2 + l_i^2\right)^{3/2}}{3d_i l_i} - d_i,$$

$$l_i = \frac{8D_i}{\pi\bar{c}_i}, \qquad C_c(d_i) = 1 + \frac{\lambda}{d_i}\left[2.514 + 0.800e^{-0.55\frac{d_i}{\lambda}}\right].$$

Here, with some algebra, it can be seen that the nominator of Equation (3.4) is equal to the continuum regime expression in Equation (3.3). Thus the denominator can be thought of as a correction to the continuum collision frequency function. Also it is easily seen that (3.4) reduces to the free molecular collision frequency function in (3.3) when d_i and d_j are both very small. To get a better feeling of how the collision frequency function depends on the particle size, it is plotted in Figure 3.1.

From Figure 3.1. it can be seen that for equally sized particles, the collision efficiency function β has a maximum at about 0.05 μm. For large particles the value of β is low because of their low Brownian diffusivities. Very small particles have high Brownian diffusivities, but the target areas for collisions are very small. Finally, it is seen that β is much larger for a collision of two unequally sized particles than for particles of equal size.

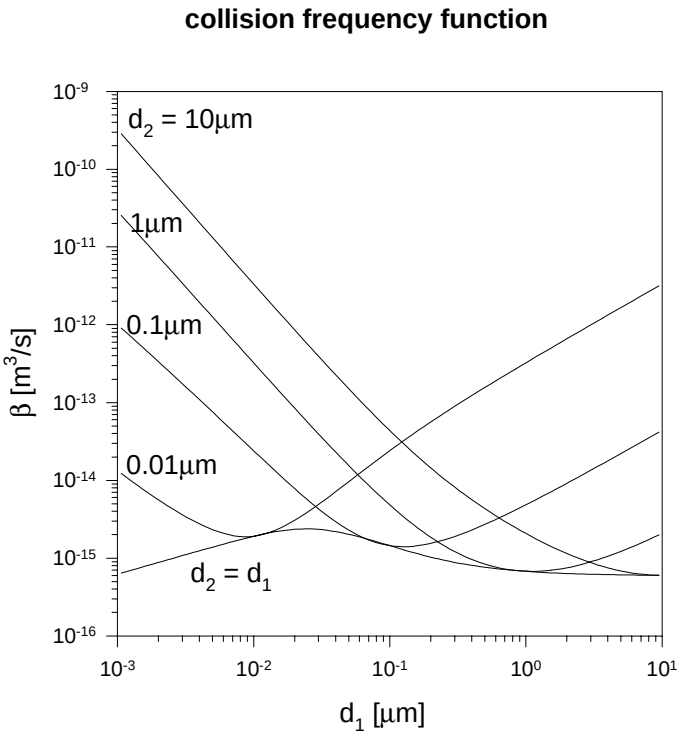

Figure 3.1. Brownian collision frequency function $\beta(d_1,d_2)$ for spherical particles of density 1000 kg/m^3 in air at 293 K and 1 atm using Equation (3.4).

3.3. Kinematic agglomeration

In Brownian agglomeration, particles collide because of their different velocities caused by random Brownian motion. If the velocity difference that is the reason for collisions is caused by external forces (gravitation, electrical forces etc.), the process is called kinematic agglomeration. A common example of kinematic agglomeration is the process of collisions of raindrops with atmospheric aerosol particles. The large raindrops have a larger terminal settling velocity than the much smaller particles. Thus, the falling raindrops sweep the area below them, collecting many of the particles in their way.

The collision frequency function for kinematic agglomeration of particles with diameters d_1 and d_2 is usually written in the following form:

$$\beta(d_1,d_2) = \varepsilon(d_1,d_2)\frac{\pi}{4}(d_1+d_2)^2|v_1-v_2|, \qquad (3.5)$$

where $|v_1 - v_2|$ is the relative velocity between the particles. The meaning of the collision efficiency $\varepsilon(d_1,d_2)$ is evident from Figure 3.2. If the particle moving with greater velocity would sweep all particles that are in its geometrical path, ε would be 1. This is, however, not the case because of the curved streamlines around the particles.

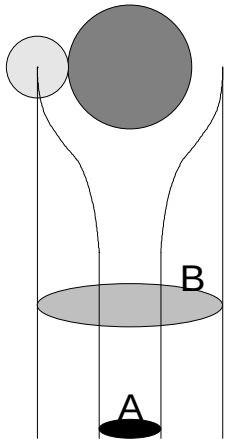

Figure 3.2. The collision efficiency ε is defined as the ratio of the effective collision cross-section to the geometrical collision cross-section ε = A/B.

For gravitational sedimentation it is possible to derive an analytical expression for ε that assumes Stokes flow and negligible inertia of the smaller particle (Pruppacher and Klett, 1978):

$$\varepsilon(d_1, d_2) = \frac{1}{2}\left(\frac{d_1}{d_1 + d_2}\right)^2; \quad d_1 << d_2 . \tag{3.6}$$

This means that with significant differences in particle sizes, the collision efficiency will be much lower than unity. If the external force is an electric field and Coulombic forces must be accounted for, the situation becomes more complicated. This problem is discussed in more detail in Chapter 4.

3.4 Agglomeration of non-spherical particles

If the particles that collide are solid and do not have enough time to coalesce before recolliding, fractal-like structures start to form. They are typically built from small almost spherical and equal-sized units, called primary particles. Such structures are conveniently described by a power-law relationship:

$$N = \frac{v}{v_0} = A\left(\frac{r}{r_0}\right)^{D_f} \tag{3.7}$$

where D_f is the fractal dimension. Equation (3.7) gives the average number of primary particles N of radius r_0 in an agglomerate of volume v and characteristic radius r (typically radius of gyration or mobility radius). For a dense structure with spherical shape D_f = 3, the factor A is found to be nearly constant and of the order unity (Wu and Friedlander, 1993a). Both experiments and numerical simulations have shown that Brownian movement dominated agglomeration processes tend to produce agglomerates with a fairly low fractal dimension, in the range $1.6 < D_f < 2.2$. It is obvious that such open structures collide and thus grow much more rapidly than spherical particles of the same volume, especially in the free molecular regime.

In the continuum regime, the effects of increased collision cross-section and decreased Brownian mobility approximately cancel each other out and thus there is not much effect on the collision frequencies (Koch and Friedlander, 1990). At present, there is no generally accepted expression available for the collision frequency function of fractal-like agglomerates. However, a first approximation can be obtained by replacing d_i in Equation (3.4) by $2r_0\left(v_i/v_0\right)^{1/D_f}$ (assuming A ≈ 1). Then we make the very strong assumption that the same characteristic diameter d_i describes both the mobility and capture properties of an agglomerate of any size.

In the free molecular and continuum limits this results in the following collision frequency functions (Matsoukas and Friedlander, 1991):

$$\beta(u,v) = \begin{cases} \dfrac{2kT}{3\mu}\left(\dfrac{1}{u^{1/D_f}} + \dfrac{1}{v^{1/D_f}}\right)\left(u^{1/D_f} + v^{1/D_f}\right); & \text{continuum} \\ & \text{regime} \\ \left(\dfrac{3}{4\pi}\right)^{2/D_f - 1/2} r_0^{\,2-6/D_f}\left(\dfrac{6kT}{\rho_p}\right)^{1/2}\left(\dfrac{1}{u} + \dfrac{1}{v}\right)^{1/2}\left(u^{1/D_f} + v^{1/D_f}\right)^2; & \\ & \text{free molecular regime} \end{cases} \tag{3.8}$$

3.5. Self-preserving solution to the agglomeration equation

Friedlander and Wang (1966) pointed out that if the collision frequency function is a homogenous function of degree n, that is if

$$\beta(\lambda u, \lambda v) = \lambda^n \beta(u, v) \tag{3.9}$$

then the transformation

$$\begin{cases} \eta = \dfrac{v}{\bar{v}(t)} \\ \bar{v}(t) n(v,t) = N(t) \psi(\eta) \end{cases} \tag{3.10}$$

reduces the agglomeration equation (3.2) to an ordinary integro-differential equation for ψ of η. This solution is called the self-preserving solution of the agglomeration equation. It is an asymptotic solution $\psi(\eta)$ towards which all systems converge, regardless of the initial distribution. It is easily checked that the collision frequency functions for the free molecular and continuum regimes (3.3) or (3.10) are homogenous functions but the Fuchs equation for the complete size spectrum (3.4) is not. If we wish to have a general solver of the coagulation equation (3.2) for all possible particle size ranges, we must use a discretization of the particle size spectrum and a numerical solution as with the complete GDE, explained in Chapter 2. The form of the self-preserving solution may be obtained by solving the coagulation equation numerically up to the point where the size distribution, expressed in the form $\psi(\eta)$, remains fixed with some preset accuracy.

The free-molecular case will now be analyzed in more detail. By inserting the free-molecular collision frequency function from (3.8) into the agglomeration equation (3.2) and by integrating the equation from 0 to ∞, we get an equation for the total particle concentration $N(t)$. This can be written in terms of the normalized variables (3.10) for the average agglomerate volume $\bar{v}$ to give (Matsoukas and Friedlander,1991; paper E)

$$\frac{d\bar{v}}{dt} = \frac{1}{2} \alpha \sqrt{\frac{6kT}{\rho}} \left(\frac{3\bar{v}}{4\pi} \right)^{1/6} \phi n^{2/D_f - 2/3} \tag{3.11}$$

Here ϕ is the volume fraction of particulate matter (volume of particles/volume of gas), n the average number of primary particles in an agglomerate and α a constant, which depends on D_f approximately by the following equation:

$$\begin{aligned} \alpha &= \int_0^\infty \int_0^\infty \left(\eta_1^{-1} + \eta_2^{-1} \right)^{1/2} \left(\eta_1^{1/D_f} + \eta_2^{1/D_f} \right)^2 \psi(\eta_1) \psi(\eta_2) d\eta_1 d\eta_2 \\ &\approx 6.548 + 112.1 \cdot D_f^{-7.883} \end{aligned} \tag{3.12}$$

Correlation (3.12) was obtained by solving the self-preserving distribution $\psi(\eta)$ numerically for different values of (constant) D_f, then integrating numerically and curve-fitting. Equation (3.11) shows the power of the self-preserving analysis: For systems in the free-molecular regime that have evolved for a sufficiently long time, the complete size distribution is described by a single ordinary differential equation (3.11) for the average agglomerate volume. A similar analysis can be carried out for the continuum regime (Wu and Friedlander, 1993b; Vemury and Pratsinis, 1995).

4. ELECTRICAL AGGLOMERATION

In removing flue gas particles at coal fired power plants, the efficient collection of particles in the diameter range 0.1 to 1.0 μm remains to be solved. The most commonly used flue gas cleaner under these circumstances is the electrostatic precipitator (ESP). According to the studies of Mohr et. al (1996), the total mass collection efficiency with the ESP can be over 99.7 %, while the collection efficiency for the above mentioned range can be only 85 %.

Much research has been done recently to solve this problem of significant submicron penetration by utilizing a particle agglomerator before the ESP in order to shift the particle size distribution in such a way that the resulting particles can be efficiently collected (Eliasson and Egli, 1991, Kobashi, 1979). The possibility of accomplishing this by using particle charging and an alternating electric field was studied in papers B and C and is briefly reviewed here. In the alternating electric field the particles start to oscillate with amplitudes and velocities depending on particle size and charging. The different velocities cause kinematic coagulation between the particles, hopefully removing most of the particles in the problematic size range.

In the experimental part of the project (paper B), unipolar charging was used. In the theoretical treatment (paper C), however, studies were extended to take into account bipolar charging as well. The experimental work was later extended to agglomeration studies of bipolarly charged particles by Laitinen (1994) and Hautanen (1995).

4.1. Parallel plate agglomerator

The basic idea of the agglomerator is simple (Figure 4.1). First, the particles are charged unipolarly with a corona charger, after which they start to oscillate in the alternating electric field of the agglomerator. Larger particles have larger oscillation amplitudes and velocities than the smaller ones, which is supposed to make them collide with each other. The experimental system is presented in detail in paper B.

The Brownian agglomeration mechanism is too weak in this system to remove the submicron particles by collisions with the large supermicron particles, especially since the unipolar charging makes the effect weaker. The aim of this setup is to remove the submicron particles by kinematic coagulation, caused by the oscillating motion. To measure this effect, the particle size distribution is measured after the agglomerator with the alternating electric field on and off. Comparing the results enables us to

separate the effect of the field from all other particle removal mechanisms in the system (Brownian agglomeration, deposition).

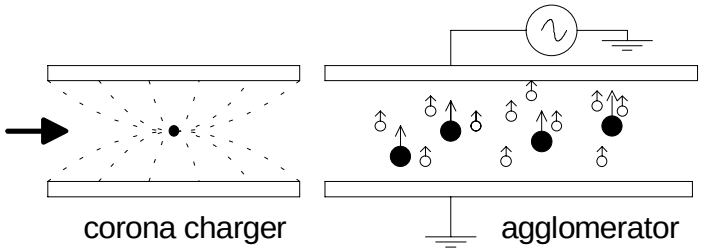

Figure 4.1. Principle of agglomeration (here the case of unipolar charging): Charged particles start to oscillate in the alternating electric field. The amplitude and velocity differences cause collisions.

The laboratory agglomerator (Paper B) had the following characteristics:

- amplitude of electric voltage E_0 = 710 000 V/m
- frequency of voltage f = 50 Hz
- residence time in agglomerator τ = 4 - 6 s
- total mass concentration of particles M = 1 - 2 g/m^3
- geometric number mean diameter of fine particle mode $\bar{d}_1$ = 0.35 um
- geometric mass mean diameter of large particle mode $\bar{d}_2$ = 3.0 um
- reduction in fine mode concentration Φ = 3 - 8 %.

In the charger, the particle aquires a charge approximately proportional to its surface area

$$q(d) = bd^2 \tag{4.1}$$

where b is 7.9·10^{-6} C/m^2. This means that a particle of 0.14 μm will have approximately 1 elementary charge, a particle of 0.45 μm 10 elementary charges, a particle of 1.4 μm 100 elementary charges and so on. The quadratic dependence of particle diameter agrees qualitatively with field charging theory (Hinds, 1982). In the following calculations, Equation 4.1 will be used for all particle sizes even if fractions of elementary charges are impossible.

4.2. Effect of Coulomb forces on Brownian agglomeration

It is possible to derive an expression for the collision frequency function, taking into account Coulomb forces between the particles (Fuchs, 1964). The procedure results in a convenient equation where the effect of the

electric charges can be expressed as a correction factor relative to the neutral case:

$$\beta_{Coul}\left(d_i, d_j\right) = \frac{\xi}{e^{\xi} - 1}\beta\left(d_i, d_j\right), \tag{4.2}$$

$$\xi = \frac{q_i q_j}{2\pi\varepsilon_0 kT\left(d_i + d_j\right)}. \tag{4.3}$$

The term ξ represents the ratio of the electrostatic potential energy at contact to the thermal energy kT. The value of the correction term is plotted in Figure 4.2 for the parameter values mentioned in the last section.

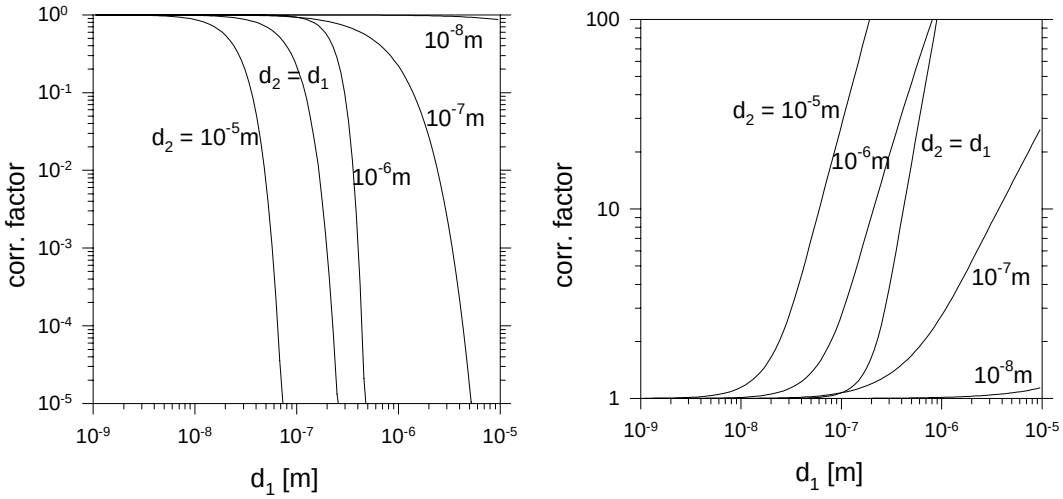

Figure 4.2. Correction factor for the Brownian collision frequency function, caused by Coulomb repulsion (left picture)/attraction (right picture).

4.3. Kinematic agglomeration of particles in an alternating electric field

If the charge of a particle is proportional to its surface area (Equation 4.1), it can easily be seen (Paper C) that the motion of the particle (diameter d) in an alternating electric field (field strength $E_0\cos(2\pi ft)$, frequency f), perpendicular to the gas flow can be described approximately with

$$x = -\frac{bE_0 d}{6\pi^2 \mu f}\sin(2\pi f t), \tag{4.4}$$

$$\dot{x} = -\frac{bE_0 d}{3\pi\mu}\cos(2\pi f t). \tag{4.5}$$

Now we see the cause of collisions. The amplitude of oscillation (and also velocity) is linearly dependent on the particle diameter. Hence the large particles have larger oscillation amplitudes and velocities than the small ones.

In the electrical agglomeration study we are interested in the case where the particles can be clearly divided into large (diameter > 1μm) collector particles and fine particles (diameter < 1 μm). To find out how effective the agglomeration process is, we must find out the volume that the large particles sweep, thus collecting the fine particles that are in their way (Paper C). This can also be conveniently approximated by using the coagulation equation (3.2) with the kinematic collision frequency function (3.5). If the number distribution of the fine particle mode is $n_1(d_1)$ and of the supermicron mode $n_2(d_2)$, the equation

$$\frac{dn_1(d_1)}{dt} = -n_1(d_1)\int_0^\infty \beta(d_1, d_2) n_2(d_2) dd_2, \tag{4.6}$$

is obtained, where the kinematic collision frequency function is

$$\beta(d_1, d_2) = \varepsilon(\sigma, d_1, d_2)\frac{\pi}{4}(d_1 + d_2)^2 \frac{2}{\pi}\frac{bE_0(d_2 - \sigma d_1)}{3\pi\mu}. \tag{4.7}$$

Here we have used the time average velocity difference of the sinusoidal motion for the term $|v_1 - v_2|$ in Equation 3.5. The constant σ takes into account three possible charging cases:

$$\sigma = \begin{cases} 1, & \text{unipolar charging} \\ -1, & \text{bipolar charging} \\ 0, & \text{neutral fine particles} \end{cases} \tag{4.8}$$

In paper B, only unipolar charging is studied. However, the same formalism is easily applied to bipolar charging and the case of neutral, non-oscillating small particles too. Equation (4.6) can now be solved for $n_1(d_1)$, thus the reduction in concentration of particles of diameter d_1 is ($m_2(d_2)$ is the mass concentration of the supermicron mode):

$$\Phi(d_1) \approx 1 - \exp\left(- \frac{bE_0\tau}{\pi^2 \rho\mu} \int_{d_2} \varepsilon(\sigma, d_1, d_2) \cdot m_2(d_2) \frac{(d_2 - \sigma d_1)(d_1 + d_2)^2}{{d_2}^3} \delta d_2 \right). \tag{4.9}$$

An important part of the theoretical study of kinematic coagulation is the determination of the collision efficiency $\varepsilon(\sigma,d_1,d_2)$ of two colliding droplets. The collision efficiency is defined as the ratio of the effective collision cross-section to the geometrical collision cross-section (Figure 3.2). The analytical expressions of Fuchs (1964) and Pruppacher and Klett (1978) for the collision efficiency in the case of gravitational coagulation are no longer valid in the case where interparticle electrical forces are important.

The determination of collision efficiencies between raindrops and aerosol particles in the atmosphere was an active research topic among cloud physicists in the late ’60s and early ’70s (Pruppacher and Klett, 1978). In most of these studies the equations of motion of the small aerosol particles are integrated into the flow field generated by the falling motion of the larger raindrops. By using a similar technique, the following equations are obtained by curve fitting into numerical results (Paper C):

$$\varepsilon(d_1, d_2) = \begin{cases} 0, \quad \text{unipolar charging } (\sigma = 1) \\ \dfrac{d_1}{d_2} + \dfrac{3}{2} \dfrac{d_1 {d_2}^2}{(d_1 + d_2)^3} \cdot \dfrac{b}{b_0} \left(1 + \dfrac{b}{10 b_0} \right), & \text{bipolar charging } (\sigma = -1) \\ \dfrac{3}{2} \left(\dfrac{d_1}{d_1 + d_2} \right)^2 & \text{neutral small particles } (\sigma = 0) \end{cases}, \tag{4.10}$$

Here b is a constant for the charge distribution (4.3) and b_0 the ”reference value” $b_0 = 7.9 \cdot 10^{-6}$ C/m^2 from the experiments (Paper B).

The curves are plotted in Figure 4.3 for different values of b/b_0. Now, if the collision efficiency $\varepsilon(d_1,d_2)$ from equation (4.10) is inserted into Equation 4.9, the reduction in the submicron mode particle concentration for a given mass distribution $m_2(d_2)$ is readily obtained. Some sample calculations are done in Paper C.

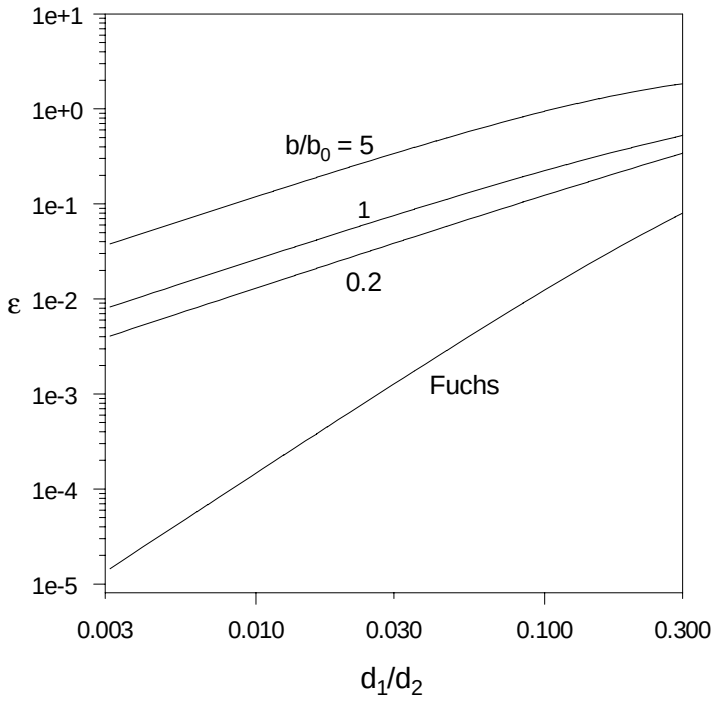

Figure 4.3. Collision efficiencies of bipolarly charged ($|q(d_i)| = bd_i^2$) particles and the Fuchs collision efficiency for the case of neutral fine particles.

4.4 Discussion

Based on the results of the previous section, unipolar kinematic agglomeration in an alternating electric field is negligible, when the fine particles to be collected and the large collector particles are charged with the same polarity. In the experiments, however, (Paper B) some reduction in the fine particle mode number concentration was observed. There are a few possible reasons for this that were not taken into account in the model.

Firstly, a small fraction of the fine particles deposit on the agglomerator walls because of their vibrating motion in the electric field. Secondly, the charge distribution (4.1) is based on an experiment that measures the average charge of the particles. This means that there are particles that have a larger charge than (4.1) and those which are neutral or even of opposite polarity. Thirdly, the electric field induces some polarization within the particles, which increases the rate of Brownian collisions (Fuchs; 1964).

Finally, the sinusoidal motion of the large and small particles is not exactly in the same phase because of the inertia of the large particles (Paper C). This means that in a short time interval, particles of the same polarity move in opposite directions, which increases the collision efficiency dramatically. Since it is already obvious from the simple theoretical analysis of the previous sections and the experimental results that unipolar charging with a subsequent alternating electric field will not be the solution for enhancing available particle removal methods, a more detailed analysis, taking into account all of the above mentioned effects, was not performed in this study.

The case of bipolar charging seems promising in terms of particle removal efficiency. The sample calculations of Paper C show that, if the collector particles and fine particles are of opposite polarity, significant reductions in the fine particle mode concentrations can be obtained. In addition, since this analysis considered only kinematic agglomeration, the fine particle reduction should be even higher because of enhanced Brownian collisions (see Figure 4.2). There is experimental evidence suggesting that actually it is the enhanced Brownian agglomeration that could be used as the fine particle removal mechanism - no electric field is needed. (Eliasson and Egli, 1991; Hautanen, 1995)

5. COALESCENCE OF AEROSOL PARTICLES

As was already briefly mentioned in the introduction to Chapter 3, the rate of coalescence is important in determining the characteristics of the collision processes. By coalescence we mean here the rounding of initially two distinct particles into one spherical particle. If coalescence is fast, only spherical particles are encountered - then the collision-coalescence process is called coagulation. If coalescence is slow, dendritic structures form and the process is called agglomeration.

In the ceramics community, the coalescence process is usually called sintering. In this context coalescence or sintering means the production of a ceramic material by heating a powder. Upon heating, the particles in the powder bond to one another yielding a higher strength. The temperature required for coalescence to become evident is typically above one half of the absolute melting temperature (German, 1996). The industrial interest in sintering results from the change of many physical properties (for example: strength, conductivity and corrosion resistance) accompanying particle bonding.

The first quantitative models of coalescence were presented by Frenkel (1945) and Kuczynski (1949). Most of the work since, reviewed nicely by Kingery et al. (1976), Coblenz et al. (1980) and German (1996), is based on their original formalism. This chapter will first briefly introduce the widely used initial and final stage coalescence models and then summarize the work of papers D, E and F concerning the modeling of simultaneous agglomeration and coalescence. Finally, the gas-to-particle aerosol route to controlled particle production is introduced. The ability to control the particle size in superfine particle production is essential because of the size dependence of many important material properties (Ichinose et al., 1992).

5.1. Initial solid state coalescence models

Here the system of interest consists of two separate spherical particles of radius r, initially touching each other. The reduction in surface free energy is the driving force for coalescence, the result of which being a single spherical particle. The purpose of this chapter is to discuss the modeling of the initial stages of sintering, i.e. the formation and growth of a neck between the particles.

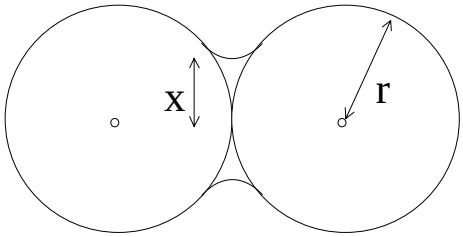

Figure 5.1. Neck formation between two spherical particles during the initial stages of coalescence.

In classical sintering models (Coblenz et al., 1980) the growth of the neck radius x (see Figure 5.1) by a single coalescence mechanism can be described with the equation

$$\left(\frac{x}{r}\right)^n = \frac{C(T)}{r^m} t \tag{5.1}$$

where $C(T)$ is a function that for a specific material and coalescence mechanism depends only on temperature (Table 5.1). The parameters m and n are constants that have different values for different coalescence mechanisms (Table 5.1).

Table 5.1. Initial neck growth model parameters for various coalescence mechanisms.

Coalescence mechanism	C(T)	m	n
viscous flow	$\frac{3\sigma}{2\mu}$	1	2
evaporation-condensation	$\frac{6\sigma p M^{3/2}}{\sqrt{2\pi}\rho^2 (RT)^{3/2}}$	2	3
lattice diffusion	$\frac{64 D_l \sigma M}{\rho RT}$	3	4
surface diffusion	$\frac{225 \delta D_s \sigma M}{\rho RT}$	4	5
grain boundary diffusion	$\frac{192 w D_b \sigma M}{\rho RT}$	4	6

σ = surface energy
μ = viscosity
p = pressure
M = molar mass
R = gas constant
T = temperature
δ = surface layer thickness
w = grain boundary width
ρ = density
D = diffusion coefficient (l = lattice, s = surface b = grain boundary)

The expression (5.1) for neck growth is based upon simplified geometries for the growing neck that limits its applicability to a neck radius below about $x/r < 0.3$. Even if the whole coalescence process cannot be described in this way, an estimate of the order of the time needed for complete coalescence (characteristic time for coalescence or fusion) can be obtained:

$$\tau_f = \frac{r^m}{C(T)}. \tag{5.2}$$

In addition, Equations 5.1 and 5.2 give us a feeling for how the coalescence process proceeds and depends on particle size. From Equation 5.1 it is clear that the neck grows rapidly at first and then the process slows down. This will be discussed in more detail in the next section. From Equation 5.2 (and Table 5.1) it is also obvious that coalescence takes longer for larger particles. For coalescence by viscous flow the characteristic coalescence time τ_f is proportional to the particle radius, and for the evaporation-condensation and diffusion mechanisms the effect is even stronger.

5.2. Coalescence models for the final stages

In their numerical simulations of coalescence by viscous flow, Hiram and Nir (1983) found that the neck radius x approaches its final value x_{sph} exponentially:

$$\frac{dx}{dt} = -\frac{1}{\tau_f}\left(x - x_{sph}\right). \tag{5.3}$$

This equation was found to hold beyond the very short time interval during which approx. 10% of the neck growth takes place.

Koch and Friedlander (1990) noted that an equation of the same form is then valid for the surface area reduction in the final stages of coalescence:

$$\frac{da}{dt} = -\frac{1}{\tau_f}\left(a - a_{sph}\right) \tag{5.4}$$

where a is the total surface area of the coalescing pair of particles and a_{sph} is the surface area of a spherical particle of the same volume. This result was already theoretically derived by Frenkel (1945) for coalescence by viscous flow and later by Friedlander and Wu (1994) for coalescence by solid state diffusion. Their derivation was based on a solution for the diffusion

equation inside the particle using spherical harmonics, with a boundary condition relating the curvature and difference in pressure across the surface. Their derivation resulted in the following form for the characteristic coalescence time, which is of the same functional form as the time in Table 5.1, differing only by a constant factor of 4:

$$\tau_f = \frac{3kTv}{64\pi D\sigma v_m} \tag{5.5}$$

where T is the absolute temperature, v the particle volume, D the solid state diffusion coefficient, σ the surface energy and v_m the molecular volume. Solid state diffusion is a thermally activated process and its temperature dependence can be represented by an Arrhenius form (Kingery et al., 1976):

$$D(T) = D_0 \exp\left(-\frac{E_{act}}{kT}\right). \tag{5.6}$$

Even if Equation (5.4) is valid only for the final stages of coalescence, it is frequently used to model the complete coalescence process because of its convenient form, which becomes especially evident in studying systems where coalescence is accompanied by simultaneous collisions with other particles. The error of this assumption is discussed in Koch and Friedlander (1990).

5.3. Simultaneous collision and coalescence

A convenient but simple technique to describe nonspherical particle dynamics is to choose the surface area in addition to the volume as particle size and shape variables. Let $n(v,a,t)$ be the particle number concentration per unit mass of gas in a volume range between v and v+dv and an area range between a and a+da at time t. In the absence of condensation and dilution by mixing, the general dynamic equation for the continuous size distribution function becomes (Koch and Friedlander, 1990)

$$\begin{aligned}
&\frac{\partial n}{\partial t} + \frac{\partial}{\partial a}\left(n\frac{\partial a}{\partial t}\right) = \\
&\frac{1}{2}\int_0^v \Theta\left[a > a_{sph}(v') + a_{sph}(v'-v)\right]\int_0^a \beta(v', v-v', a', a-a')n(v', a') \\
&\qquad\qquad n(v-v', a-a')da'\,dv' \\
&-n(v,a)\int_0^\infty \int_0^\infty \beta(v,v',a,a')n(v',a')da'\,dv'
\end{aligned} \tag{5.7}$$

The collision frequency function β is assumed to be a function of particle volume and area only. The second term of Equation 5.7 represents the motion in area space due to coalescense. The right hand side is the change due to collision. The step function Θ is required because the surface area of the particle produced by a collision is greater than the sum of the minimum surface areas $a_{\mathrm{sph}}(v)$ of the two original particles.

Using the exponential decay law for the surface area (Equation 5.4), multiplying by a and integrating with respect to a and v (Paper D), the following linear relationship for the total surface area per unit volume A_{sph} of all aerosol particles is obtained:

$$\frac{dA}{dt} = -\frac{1}{\tau_f(\bar{v})}\left(A - A_{sph}\right) \tag{5.8}$$

where A is the total surface area per unit mass of gas, $\bar{v}$ is the average particle volume and A_{sph} is the minimum possible surface area (complete coalescence) per unit mass of gas.

It is convenient to introduce a new variable θ (Paper D), which represents the fractional deviation of the aerosol surface area from the state in which each particle has relaxed to the spherical shape:

$$\theta = \frac{A - A_{sph}}{A_{sph}}. \tag{5.9}$$

Using θ as the surface area variable transforms equation 5.8 into the following form:

$$\frac{d\theta}{dt} + \left[\frac{1}{\tau_f(\bar{v})} - \frac{1}{\tau_c(\bar{v})}\right]\theta = \frac{1}{\tau_c(\bar{v})}, \tag{5.10}$$

where τ_c is the characteristic collision time, defined by

$$\frac{1}{\tau_c} = -\frac{1}{A_{sph}}\frac{dA_{sph}}{dt} = \frac{1}{3\bar{v}}\frac{d\bar{v}}{dt}. \tag{5.11}$$

Studying this form of the equation gives a deeper insight to the problem of simultaneous collisions and coalescence, at least in a cooling system. This is due to the exponential nature of equation 5.10, in which the sign of the

factor before θ determines the nature of the solution (see paper D). At the beginning, when the temperature is high, the characteristic coalescence time τ_f is shorter than the characteristic collision time τ_c. Then θ will stay close to zero. When the temperature falls, the solid state diffusion coefficient decreases very rapidly and at some point τ_f becomes greater than τ_c. Thus, the nature of the solution changes and θ starts to grow rapidly. This is approximately the point at which the primary particle size is determined, and dendritic agglomerate stuctures start to form.

In some applications, much of the primary particle growth may occur within large agglomerates. As the linear coalescence law (equation 5.4) is strictly valid only for the final stages of coalescence, it is not expected to work well for the coalescence of large agglomerates (of *n* primary particles). In paper E, the applicability of the linear coalescence law is extended by applying it to smaller domains (of *m* primary particles) of the agglomerate, instead of the complete dendritic structure. By doing so, the following approximate equations are obtained for the growth of the average agglomerate and primary particle sizes:

$$\frac{dv_a}{dt} = \frac{1}{2}\alpha\sqrt{\frac{6kT}{\rho}}\left(\frac{3v_a}{4\pi}\right)^{1/6}\phi n^{2/D_f - 2/3} \tag{5.12}$$

$$\frac{dv_p}{dt} = \begin{cases} \dfrac{64\pi D\sigma v_0}{kT}\left(m^{-1} - m^{-4/3}\right), & n = \dfrac{v_a}{v_p} > m \\ \dfrac{64\pi D\sigma v_0}{kT}\left(n^{-1} - n^{-4/3}\right), & n = \dfrac{v_a}{v_p} \le m \end{cases} \tag{5.13}$$

Equations 5.12 and 5.13 are coupled through $n = v_p/v_a$, the value of which also determines which right-hand-side is used equation 5.13. Although approximate, equation 5.13 is intuitively correct in the sense that it reduces to equation 5.8 if *n* is small, and does not depend on *n* if *n* is large. Equation 5.13 can be actually thought of as an interpolation between the two extreme cases.

5.4 Gas-to-particle aerosol technique for controlled nanoparticle production

The unique properties of matter comprised of superfine structures have raised a lot of attention in recent years (Ichinose et al. 1992, Siegel 1994). Aerosol techniques provide a useful tool to produce high purity materials in a controlled way (Pratsinis and Kodas, 1993). In the gas-to-particle aerosol conversion process, precursor vapors react and form product particles that grow further by collisions. Powders made by such techniques typically have narrow size distributions and they consist of nonporous, spherical primary particles. The gas-to-particle route for material synthesis is used on an industrial scale, for example, in the production of pigmentary titania and fumed silica.

High temperatures are usually required for the reaction of the precursor vapor to produce molecules of the desired material. These molecules grow by condensation or coagulation, retaining a spherical form if the collision rate is slower than the coalescence rate. In the opposite situation, agglomerates of spherical primary particles form. The high temperatures required for the reaction are obtained typically in flame, furnace, plasma or laser reactors.

An example of the gas-to-particle aerosol technique for nanophase material production is the free jet described in paper F (Figure 5.2). The system consists of a precursor vapor introduced as a jet into a methane-air flame, in which the precursor reacts with oxygen to form metal oxide particles. The particles grow by simultaneous collision and coalescence, the rates of which determine the final primary particle size (papers D-G). The particle size is controlled by using temperature, residence time and volume loading as control parameters. The effect of material properties, especially the solid state diffusion coefficient, is studied by performing the experiments with three different materials: Titania, Alumina and Niobium Oxide. Based on comparisons with model calculations it is obvious that even simple models based on characteristic time scales can give valuable information on how the process parameters affect the dynamics of the material synthesis process (Paper G).

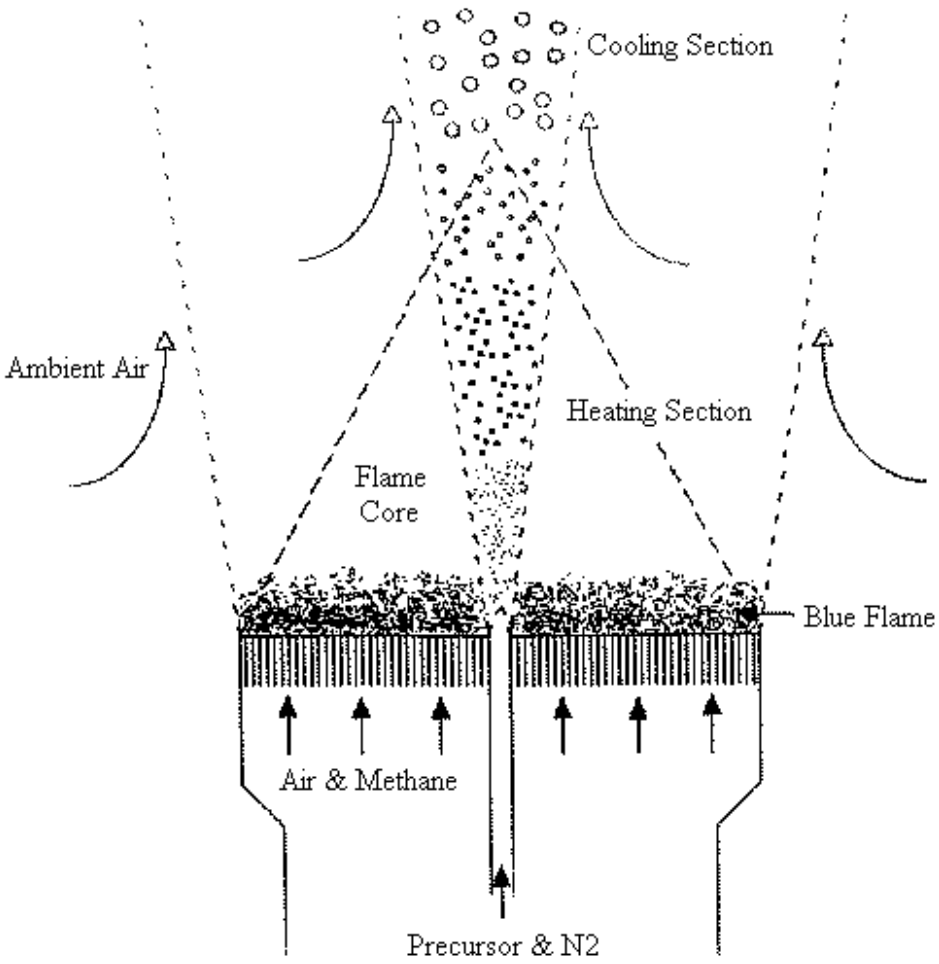

Figure 5.2. The free jet material reactor is comprised of a precursor-nitrogen jet, brought into a methane-air flame. Particles grow along the jet axis until coalescence is quenched by ambient air.

6. CONCLUSIONS

In this thesis, theoretical modeling of certain aerosol systems has been presented. After starting from aspects of a general aerosol dynamics solution routine, the focus of the thesis considers two applications, in which particle collisions are the dominating dynamic mechanism and simple, almost analytical theoretical models are within reach.

The first application is the electrical agglomerator, in which aerosol particles are charged and brought into an alternating electric field. With this arrangement the aim is to remove submicron particles from flue gases by collisions with larger particles before conventional gas cleaning devices that have a clear penetration window in the problematic 0.1-1 μm size range. A model was derived for the removal of the submicron particles in an agglomerator, in which the effect of electric charge on the collision efficiencies was computed numerically.

The theoretical analysis performed clearly demonstrates that bipolar charging is necessary to obtain significant removal of submicron particles by such an arrangement. Optimally, the particles to be collected and the larger collector particles should have opposite charges. The efficiency of bipolar charging comes from two effects: 1) the motion of oppositely charged particles in an alternating electric field is in opposite phase and 2) oppositely charged particles attract each other.

The second application is controlling nanoparticle size in the gas-to-particle aerosol route to material synthesis. In a typical material reactor, a precursor vapor reacts to form molecules of the desired material. In a cooling environment, a particulate phase forms, in which the particles grow by collisions. At first, the collision rate is slower than the coalescence rate - thus the particles remain spherical. The coalescence rate is a strong function of temperature, and at some point the collision rate becomes faster. This is where agglomerate stuctures start to form and approximately the point which determines the primary particle size. These stages were demonstrated using a laboratory scale free jet material reactor.

A theoretical model based on the simultaneous solution of collision and coalescence is presented, which is based on the self-preserving solution to the agglomeration equation and solid state coalescence models. It gives the average agglomerate size and primary particle size as a function of location in a given material reactor. Consequently, the onset of dendrite formation and final primary particle size of the produced material are also predicted.

From the comparisons between theory and experiment it is obvious that such a model is able to capture the effects of the system parameters (temperature, velocity, volume loading of material and location of collection) on the primary particle size of the produced material, and can thus be a valuable tool in producing nanomaterials of desired properties.

REFERENCES

Coblenz, W. S., Dynys, J. M., Cannon, R. M. and Coble, R. L. (1980). Initial solid state sintering models. A critical analysis and assessment. Sintering Processes, Material Science Research 13, pp. 141 - 157.

Eliasson, B. and Egli, W. (1991). Bipolar coagulation - modeling and applications. J. Aerosol Sci. 22, pp. 429 - 440.

Frenkel, J. (1945). Viscous flow of crystalline bodies under the action of surface tension. Journal of Physics 9, pp. 385 - 391.

Friedlander, S. K. (1977). *Smoke, Dust and Haze.* John Wiley and Sons, New York. 317 p.

Friedlander, S. K. and Wang, C. S. (1966). The self-preserving particle size distribution for coagulation by Brownian motion. J. Colloid Interface Sci. 22, pp. 126 - 132.

Friedlander, S. K. and Wu, M. K. (1994). Linear rate law for the decay of the excess surface area of a coalescing solid particle. Phys. Rev. B 49, pp. 3622 - 3624.

Fuchs, N. A. (1964). *The Mechanics of Aerosols.* Dover, New York. 408 p.

Gelbard, F. and Seinfeld, J. H. (1978). Coagulation and growth of a multicomponent aerosol. J. Colloid Interface Sci. 63, pp. 472 - 479.

Gelbard, F. and Seinfeld, J. H. (1980). Simulation of multicomponent aerosol dynamics. J. Colloid Interface Sci. 78, pp. 485 - 501.

German, R. (1996). *Sintering Theory and Practice.* John Wiley and Sons, New York. 550 p.

German, R. M. and Munir, Z. A. (1976). Surface area reduction during isothermal sintering. J. American Ceramic Soc. 59, pp. 379 - 383.

Hautanen, J. (1995). Agglomeration of charged aerosol particles. PhD Thesis, Tampere Univ. of Tech. Publications no. 158. 164 p.

Hinds, W. C. (1982). *Aerosol Technology.* Wiley Interscience, New York. 424 p.

Hiram, Y. and Nir, A. (1983) A simulation of surface tension driven coalescence. J. Colloid Interface Sci. 95, pp. 462 - 470.

Ichinose, N., Ozaki, Y. and Kashu, S. (1992). *Superfine Particle Technology.* Springer-Verlag, Berlin.

Im, K. H., Ahluwalia, R. K. and Lin, H. C. (1987). The RAFT computer code for calculating aerosol formation and transport in severe LWR accidents. EPRI Report NP-5287-CCM.

Kim, Y. P. and Seinfeld, J. H. (1992). Simulation of multicomponent aerosol dynamics. J. Colloid Interface Sci. 149, pp. 425 - 449.

Kingery, W. D., Bowen, H. K. and Uhlmann, D. R. (1976). *Introduction to Ceramics.* John Wiley and Sons, New York. 1032 p.

Kobashi, M. (1979). Particle agglomeration induced by alternating electric fields. PhD Thesis, Stanford University. 212 p.

Koch, W. and Friedlander, S. K. (1990). The effect of particle coalescence on the surface area of a coagulating aerosol. J. Colloid Interface Sci. 140, pp. 419 - 427.

Kuczynski, G. C. (1949). Self-diffusion in sintering of metallic particles. Trans. AIME 185, pp. 169 - 178.

Laitinen, A. (1994). Agglomeration of electrically charged aerosol particles. MSc Thesis, Tampere Univ. of Tech. Dept. Electrical Eng. Report 2-94. 80 p.

Matsoukas, T. and Friedlander, S. K. (1991). Dynamics of aerosol agglomerate formation. J. Colloid Interface Sci. 146, pp. 495 - 506.

Mohr, M., Ylätalo, S., Klippel, N., Kauppinen, E. I., Riccius, O. and Burtscher, H. (1996). Submicron fly ash penetration through electostatic precipitators at two coal power plants. Aerosol Sci. Tech. 24, pp. 191 - 204.

Pratsinis, S. E. and Kodas, T. T. (1993). Manufacturing of materials by aerosol processes, *in Aerosol Measurement: Principles, Techniques and Applications* (ed. Willeke, K. and Baron, P. A.). Van Nostrand Reinhold, New York. pp. 721 - 746.

Pruppacher, H. R. and Klett, J. D. (1978). *Microphysics of Clouds and Precipitation.* D. Reidel Publishing Co., Dordrecht. 714 p.

Sher, R. and Jokiniemi, J. K. (1993). NAUAHYGROS 1.0: A code for calculating the behaviour of aerosols in nuclear plant containments following a severe accident. EPRI Report TR-102775.

Schmoluchowski, M. (1917). Z. Physik. Chem. 92, pp. 129 - 154.

Siegel, R. W. (1994). Nanophase Materials: Synthesis, structure and properties, in *Physics of New Materials* (ed. Fujita, F. E.). Springer-Verlag, Berlin, pp. 65 - 105.

Vemury, S. and Pratsinis, S. E. (1995). Self-preserving size distributions of agglomerates. J. Aerosol Sci. 26, pp. 175 - 185.

Wu, J. J. and Flagan, R. C. (1988). A discrete-sectional solution to the aerosol dynamic equation. J. Colloid and Interface Sci. 123, pp. 339 - 352.

Wu, M. and Friedlander, S. K. (1993a). Note on the power law equation for fractal-like aerosol agglomerates. J. Colloid Interface Sci. 159, 246 - 248.

Wu, M. and Friedlander, S. K. (1993b). Enhanced power law agglomerate growth in the free molecule regime. J. Aerosol Sci. 24, pp. 273 - 282.